*Title page

Cannabinoid type 2 receptors mediate a cell type-specific self-inhibition in cortical neurons

Alexander Stumpf[1], Daniel Parthier[1], Rosanna P. Sammons[1], A. Vanessa Stempel[1,2], Jörg Breustedt[1], Benjamin R. Rost[1,3], Dietmar Schmitz[1,3,4,5,6,7]

Affiliations

1   Neuroscience Research Center, Charité-Universitätsmedizin Berlin, Germany

2   Sainsbury Wellcome Centre for Neural Circuits and Behaviour, University College London, UK

3   German Center for Neurodegenerative Diseases (DZNE), Berlin, Germany

4   Berlin Institute of Health, Berlin, Germany

5   Bernstein Center for Computational Neuroscience Berlin, Germany

6   Cluster of Excellence NeuroCure, Berlin, Germany

7   Einstein Center for Neurosciences, Berlin, Germany

Correspondence should be addressed to

Prof. Dr. Dietmar Schmitz

Charité - Universitätsmedizin Berlin

Charitéplatz 1; 10117 Berlin, Germany

Telefone: +49 30 450 539054

Fax: +49 30 450 539916

dietmar.schmitz@charite.de

Abbreviations: CB_1R and CB_2R, cannabinoid receptors type 1 and 2; SSI, slow self-inhibition; GIRK channel, G protein-coupled inward-rectifying K^+ channel; GPCR, G protein-coupled receptors; DSI, depolarization-induced suppression of inhibition; DSE, depolarization-induced suppression of excitation; CNS, central neural system; APs, action potentials; 2-AG, 2-arachidonoylglycerol; LTS, low –threshold spiking interneurons; NBC, sodium/bicarbonate co-transporter; PC, pyramidal cell; RSNPC, regular spiking non-pyramidal cell; FS, fast spiking interneuron; ACSF, artificial cerebrospinal fluid; V_m, membrane potential; NE, noladin ether;

Abstract

Endogenous cannabinoids are diffusible lipid ligands of the main cannabinoid receptors type 1 and 2 (CB_1R and CB_2R). In the central nervous system endocannabinoids are produced in an activity-dependent manner and have been identified as retrograde modulators of synaptic transmission. Additionally, some neurons display a cell-autonomous slow self-inhibition (SSI) mediated by endocannabinoids. In these neurons, repetitive action potential firing triggers the production of endocannabinoids, which induce a long-lasting hyperpolarization of the membrane potential, rendering the cells less excitable. Different endocannabinoid receptors and effector mechanisms have been described underlying SSI in different cell types and brain areas. Here, we investigate SSI in neurons of layer 2/3 in the somatosensory cortex. High-frequency bursts of action potentials induced SSI in pyramidal cells (PC) and regular spiking non-pyramidal cells (RSNPC), but not in fast-spiking interneurons (FS). In RSNPCs the hyperpolarization was accompanied by a change in input resistance due to the activation of G protein-coupled inward-rectifying K^+ (GIRK) channels. A CB_2R-specific agonist induced the long-lasting hyperpolarization, whereas preincubation with a CB_2R-specific inverse agonist suppressed SSI. Additionally, using cannabinoid receptor knockout mice, we found that SSI was still intact in CB_1R-deficient but abolished in CB_2R-deficient mice. Taken together, we describe an additional SSI mechanism in which the activity-induced release of endocannabinoids activates GIRK channels via CB_2Rs. These findings expand our knowledge about cell type-specific differential neuronal cannabinoid receptor signaling and suggest CB_2R-selective compounds as potential therapeutic approaches.

Abstract

Endogenous cannabinoids are diffusible lipid ligands of the main cannabinoid receptors type 1 and 2 (CB_1R and CB_2R). In the central nervous system endocannabinoids are produced in an activity-dependent manner and have been identified as retrograde modulators of synaptic transmission. Additionally, some neurons display a cell-autonomous slow self-inhibition (SSI) mediated by endocannabinoids. In these neurons, repetitive action potential firing triggers the production of endocannabinoids, which induce a long-lasting hyperpolarization of the membrane potential, rendering the cells less excitable. Different endocannabinoid receptors and effector mechanisms have been described underlying SSI in different cell types and brain areas. Here, we investigate SSI in neurons of layer 2/3 in the somatosensory cortex. High-frequency bursts of action potentials induced SSI in pyramidal cells (PC) and regular spiking non-pyramidal cells (RSNPC), but not in fast-spiking interneurons (FS). In RSNPCs the hyperpolarization was accompanied by a change in input resistance due to the activation of G protein-coupled inward-rectifying K^+ (GIRK) channels. A CB_2R-specific agonist induced the long-lasting hyperpolarization, whereas preincubation with a CB_2R-specific inverse agonist suppressed SSI. Additionally, using cannabinoid receptor knockout mice, we found that SSI was still intact in CB_1R-deficient but abolished in CB_2R-deficient mice. Taken together, we describe an additional SSI mechanism in which the activity-induced release of endocannabinoids activates GIRK channels via CB_2Rs. These findings expand our knowledge about cell type-specific differential neuronal cannabinoid receptor signaling and suggest CB_2R-selective compounds as potential therapeutic approaches.

1 Introduction

The endocannabinoid system is one of the main neuromodulatory systems in the vertebrate central nervous system (CNS). Endocannabinoids are membrane-derived lipid molecules that mainly, albeit not exclusively, exert their effects by acting via G protein-coupled receptors (GPCR) (Kano, 2009). While CB_1Rs are one of the most widely expressed GPCRs in the CNS, CB_2Rs were traditionally referred to as peripheral endocannabinoid receptors, since their expression was primarily detected in cells of the immune system (Munro et al., 1993).

The best-studies effects of endocannabinoids in the CNS are two forms of short-term synaptic plasticity: depolarization-induced suppression of inhibition (DSI) and excitation (DSE) (Kreitzer and Regehr, 2001; Ohno-Shosaku et al., 2001; Wilson and Nicoll, 2001). In both DSI and DSE, endocannabinoids are produced by the postsynaptic cell and retrogradely activate presynaptic CB_1Rs. Further, numerous forms of CB_1R-dependent synaptic long-term plasticity have been described, with endocannabinoids being involved in both long-term potentiation (Gómez-Gonzalo et al., 2015; Maglio et al., 2017; Wang et al., 2016) and long-term depression (Chevaleyre and Castillo, 2003; Gerdeman et al., 2002; Safo and Regehr, 2005; Sjöström et al., 2003). However, in recent years several publications have provided functional evidence for the presence of CB_2Rs in cells of the CNS, where CB_2Rs exert inhibitory effects (García-Gutiérrez et al., 2013, 2012; Gong et al., 2006; Kim and Li, 2015; Onaivi, 2007; Stempel et al., 2016).

In addition to their synaptic effects, a plethora of non-synaptic and cell-autonomous forms of endocannabinoid modulation exists (Bacci et al., 2004; den Boon et al., 2012; Stempel et al., 2016). For example, layer 2/3 pyramidal neurons and layer 5 low-threshold spiking (LTS) interneurons in the somatosensory cortex express a CB_1R-dependent form of self-inhibitory plasticity, namely SSI (Bacci et al., 2004; Marinelli et

al., 2009). In both cell types, trains of action potentials (APs) were described to induce the production of the endocannabinoid 2-arachidonoylglycerol (2-AG) and subsequent CB_1R activation within the same cell. This leads to a G protein-dependent opening of GIRK channels, which hyperpolarizes the cell. In contrast, in hippocampal CA3 pyramidal cells, activation of CB_2Rs has been shown to cause a long-lasting hyperpolarization of the cells that alters local network rhythms (Stempel et al., 2016). This form of self-inhibition is phenotypically similar to cortical SSI but depends on the downstream modulation of the sodium/bicarbonate co-transporter (NBC).

At present, it is not known if SSI in different types of cortical neurons exclusively depends on CB_1Rs or whether CB_2Rs may also contribute to its induction. Furthermore, it is not clear exactly which cell types are capable of inducing SSI and by which mechanism it is implemented.

In this study, we investigate cell-autonomous SSI in neocortical neurons of the mouse somatosensory cortex layer 2/3. We show that trains of APs evoke a long-lasting hyperpolarization in pyramidal cells (PCs) and regular spiking non-pyramidal cells (RSNPCs), but not in fast spiking interneurons (FS). In RSNPCs, this self-inhibition is exclusively mediated by activation of CB_2R, demonstrated both by pharmacological tools and knockout (KO) mice, and leads to a hyperpolarization via activation of GIRK channels. Our findings add to the understanding of the highly complex function of the endocannabinoid neuromodulatory system, and provide additional evidence for functional expression of CB_2R in the CNS.

3

2 Materials and Methods

2.1 Ethical Statement and Animal Handling

Animal husbandry and experimental procedures were performed in accordance with the guidelines of local authorities (Berlin, Germany), the German Animal Welfare Act, and the European Council Directive 86/609/EEC. CB_1R- and CB_2R-deficient mice (Buckley et al., 2000; Zimmer et al., 1999) were maintained on a C57BL/6n genetic background, and homozygous KO mice and their wild-type (WT) littermates were obtained from heterozygous breeding. Animals were housed on a 12:12h reversed day-night cycle with food and water *ad libitum*.

2.2 Preparation of brain slices

Coronal slices were prepared from the somatosensory cortex of C57BL6/n mice, CB_1R or CB_2R KO mice and their WT-littermates aged postnatal day 21-35. Animals were anesthetized with isoflurane and decapitated. Brains were removed and transferred to ice-cold sucrose-based artificial cerebrospinal fluid (sACSF) containing in mM: 87 NaCl, 26 $NaHCO_3$, 50 sucrose, 10 glucose, 2.5 KCl, 1.25 NaH_2PO_4, 3 $MgCl_2$, 0.5 $CaCl_2$. Tissue blocks were mounted on a vibratome (Leica VT 1200S, Leica Microsystems), cut at 300 μm thickness, and stored in an interface chamber. The interface chamber was perfused with ACSF containing in mM: 119 NaCl, 26 $NaHCO_3$, 10 glucose, 2.5 KCl, 1 NaH_2PO_4, 2.5 $CaCl_2$ and 1.3 $MgCl_2$. Slices were incubated for at least 60 min before recordings started. All ACSF solutions were equilibrated with carbogen (95% O_2 and 5% CO_2).

2.3 Slice electrophysiology

Whole-cell current-clamp recordings were performed in layer 2/3 of somatosensory cortex with a $KMeSO_3$-based intracellular solution (containing in mM: 130 $KMeSO_3$, 10

4

KCl, 10 HEPES, 4 NaCl, 4 Mg-ATP, 0.5 Na-GTP, 5 Na-Phosphocreatine, 0.1 % Biocytin), using a Multiclamp 700B amplifier (Molecular Devices). Data were low-pass filtered at 3 kHz and sampled at 10 kHz. Neurons were identified visually with infrared differential interference contract (IR-DIC) optics on an Olympus BX-51 WI microscope. Interneurons were differentiated from PCs based on two criteria: a lack of apical dendrite projecting towards the pial surface, and horizontally orientated and spherical shaped somata compared to the pyramidal shaped somata of PCs. Experiments were only performed if cells had a resting membrane potential more hyperpolarized than -55 mV (without correction for liquid junction potential) and a series resistance below 25 MΩ. Bridge balance and pipette capacitance compensation was performed throughout the recording. Cells were characterized by recording their membrane response and firing pattern by applying hyperpolarizing and depolarizing current steps (-200 to + 600 pA, increment: 40 pA, 1 s). Fast-spiking interneurons showed high frequency AP firing (>200 Hz) with no frequency adaptation. Both RSNPCs and PCs showed moderate spiking frequency (20 – 60 Hz) and increasing inter-spike intervals during the depolarization step. The AP slope ratio was calculated by dividing maximal positive slope with the maximal negative slope of the AP. Before inducing SSI, we manually adjusted the membrane potential to -60 mV by continuous somatic current injection and recorded a stable baseline for 2 min. Cells that did not reach a stable baseline were excluded. SSI was induced either by eliciting AP trains with 2 ms long somatic current injection (10 AP trains, 20 s inter-train interval; 50 APs/train at 100 Hz) or by bath application of the CB_2R agonist HU-308 (1 µM, Tocris). Other pharmacological agents (10 µM SCH23390, Tocris; 10µM S0589, Sigma-Aldrich; 1 µM SR 144528, Tocris) were applied to the bath and brain slices were preincubated for at least 10 min before recordings were performed. The input resistance was monitored by a 400 ms test-pulse of -40 pA every 20 s.

2.4 Data analysis and statistics

Data were recorded and analyzed with Igor Pro (Wavemetrics) and Neuromatic software. Changes in membrane potential (ΔV_m) were calculated by subtracting the average membrane potential of 2 min, 60 s after the last AP train, from the baseline membrane potential. Changes in input resistance after SSI were calculated by normalizing the average input resistance after SSI induction to the average baseline input resistance. Cells were classified as responsive when ΔV_m was higher than three times the standard deviation of the baseline. Sample size is given as the number of recorded cells (*n*). D'Agostino-Pearson normality test was performed to test individual datasets for normal distribution of the data points. Normally distributed datasets were compared using a two-tailed Student's t-test. Stated *p*-values refer to comparison of hyperpolarization amplitude (ΔV_m) between different datasets by using Student's t-test, unless otherwise stated. If datasets were not normally distributed a Mann-Whitney test was performed to compare the groups. Data are presented as mean ± standard error of the mean (SEM). Box plots are shown as median with 25th and 75th percentile.

2.5 Morphological reconstruction

Biocytin-containing intracellular solution (0.1 % Biocytin) was used for post-hoc identification of the recorded neuron. After the recording, the brain slices were fixed overnight in 4% paraformaldehyde in PBS (pH 7.4) at 4°C before subsequent visualization with streptavidin conjugated with Alexa-488 (RRID:AB_2315383). Stained slices were imaged with a laser confocal microscope (Leica SP5 on a Leica DMI 6000) using a 20x or 63x objective and a z-step size of 1 μm. Morphological reconstruction was performed using Neutube (Feng et al., 2015) and Fiji software (Schindelin et al., 2012).

3 Results

3.1 Cell type-specific hyperpolarization

We performed whole-cell patch-clamp recordings from different cell types of layer 2/3 in the somatosensory cortex. Based on their appearance in the IR-DIC image, we identified PCs by their eponymous soma shape and a prominent apical dendrite projecting towards the pial surface (Fig. 1A). Interneurons were differentiated by their horizontally orientated or spherical shaped somata and the absence of a prominent apical dendrite (Fig. 1B, 1C). Interneurons were further differentiated according to their firing properties (Table 1) into RSNPCs (Fig 1B) and FS interneurons (Fig. 1C). Physiological properties and firing patterns of PCs and RSNPCs were very similar (Table 1). In contrast, FS had a lower input resistance and showed a characteristic firing pattern (shorter AP half-width and high frequency firing), which allowed distinguishing these neurons from PCs and RSNPCs (Table 1).

Trains of APs elicited long-lasting SSI in PCs (Fig. 1D, G, J: ΔV_m: -4.1 ± 1.5 mV) and in RSNPCs (Fig. 1E, H, K: ΔV_m: -5.6 ± 1.1 mV), but not in FS interneurons (Fig. 1F, I, L: ΔV_m: -0.7 ± 0.5 mV).

According to our criteria (see Methods), 73 % (8/11) of PCs and 71% (15/21) of RSNPCs exhibited a significant hyperpolarization after AP trains, whereas none of the FS were responsive. Here, both responsive and non-responsive cells were included in averaged values and statistics (Fig. 1). Taken into account only responsive cells, PCs hyperpolarize by -6.0 ± 1.6 mV and RSNPCs by -7.6 ± 1.0 mV (data not shown).

Thus, trains of APs induced a long-lasting hyperpolarization exclusively in regular spiking cells (PCs and RSNPCs) in layer 2/3 of the somatosensory cortex, but not in FS interneurons. We also assessed the stability of SSI and found that the SSI induced

hyperpolarization of the membrane potential in RSNPCs was stable and lasted for the entire recording period of up to 40 min after induction (Suppl. Fig. 1A). Additional AP trains with an interval of two minutes that were applied after SSI had stabilized did not lead to any further significant additional hyperpolarization of the cells (Suppl. Fig. 1B and C).

3.2 Mechanism underlying long-lasting hyperpolarization in regular spiking non-pyramidal neurons

We have previously shown that trains of APs induce a cell-autonomous CB_2R-dependent SSI in hippocampal PCs by activation of a sodium/bicarbonate co-transporter (NBC) (Stempel et al. 2016). In contrast, both layer 2/3 PCs and layer 5 interneurons of the somatosensory cortex utilize an alternative mechanism in which activation of CB_1Rs induces a GIRK channel-driven hyperpolarization (Bacci et al., 2004; Marinelli et al., 2009).

The cellular mechanisms of SSI have not been characterized before in layer 2/3 RSNPCs, despite the fact that of all cells in layer 2/3, these show the most pronounced SSI (Fig. 1). Thus, we focused on RSNPCs to further investigate the SSI mechanism: in RSNPCs, the magnitude of hyperpolarization correlated with the decrease in input resistance (Fig. 2A), indicating an increase in ion channel conductance. Preincubation with an inhibitor of NBC (10 µM S0589) did not alter SSI in RSNPCs (ΔV_m: -4.4 ± 3.4 mV; n = 13; p = 0.4 compared to control condition; data not shown). In contrast, preincubation with a GIRK channel blocker (10 µM SCH23390) prevented the long-lasting hyperpolarization (Fig. 2B-D: control ΔV_m: -5.6 ± 1.1 mV; 15/21 responsive cells; SCH23390 ΔV_m: -0.2 ± 1.1 mV; 1/11 responsive cells). Additionally, application of SCH23390 after SSI induction strongly

depolarized the cells and increased input resistance, reversing the AP-induced effects (Fig. 2E-F). In contrast, only a weak baseline depolarization occurred when SCH23390 was applied to non-stimulated RSNPCs (Fig. 2G).

Thus, the AP-induced hyperpolarization in RSNPCs is mediated via activation of GIRK channels and not by the NBC.

3.3 CB$_2$ receptors mediate SSI

SSI was previously characterized as an endocannabinoid-dependent mechanism, in which either CB$_1$Rs (Bacci et al., 2004; Marinelli et al., 2009) or CB$_2$Rs (Stempel et al., 2016) induce a long-lasting hyperpolarization after periods of AP firing, via different mechanisms. The specific CB$_2$R agonist HU-308 (1 µM) mimicked the AP-induced hyperpolarization, whereas application of the endocannabinoid Noladin ether (NE, 300 nM), which displays selectivity for CB$_1$Rs over CB$_2$Rs (Hanus et al., 2001), did not cause a hyperpolarization (Fig. 3A and B: HU-308 ΔV_m: -6.0 ± 1.6 mV, 8/11 responding cells; NE: ΔV_m: -0.4 ± 0.8 mV, 3/10 responding cells). Additionally, preincubation with the CB$_2$R inverse agonist SR 144528 (1 µM) prevented the AP-induced long-lasting hyperpolarization (Fig. 3C and D: control ΔV_m: -5.6 ± 1.1 mV, 15/21 responsive cells; SR 144528: ΔV_m: -0.8 ± 0.6 mV, 3/15 responsive cells) indicating the involvement of CB$_2$R in SSI.

In order to verify this finding, we used transgenic KO mice lacking CB$_1$R or CB$_2$R (CB$_1$R KO and CB$_2$R KO) and their corresponding littermates (Buckley et al., 2000; Zimmer et al., 1999) to further disentangle the involvement of the major cannabinoid receptors in AP-induced SSI. In both CB$_1$R KO mice and WT-littermates, trains of APs elicited a long-lasting hyperpolarization of similar magnitude in RSNPCs (Fig. 4A – C: CB$_1$R KO: ΔV_m: -3.7 ± 0.9 mV, 12/17 responsive cells; CB$_1$R WT: ΔV_m: -5.2 ± 1.5 mV, 7/10 responsive cells). In

contrast, CB$_2$R-deficient mice showed a marked reduction of SSI, both in the SSI amplitude (Fig. 4D and E: CB$_2$R KO: ΔV_m: -0.4 ± 0.6 mV; CB$_2$R WT: ΔV_m: -3.6 ± 0.8 mV) as well as in the number of responding cells (Fig. 4F: CB$_2$R KO: 2/12; CB$_2$R WT: 9/12).

Corresponding phenotypes were also observed in recordings of PCs in transgenic CB-R knockout animals: in CB$_1$R-deficient mice and their WT littermates trains of APs induced SSI of similar magnitude (CB$_1$R WT: ΔV_m: -3.9 ± 0.9 mV; CB$_1$R KO: ΔV_m: -4.2 ± 1.5 mV; Suppl. Fig. 2). In contrast, the genetic deletion of CB$_2$Rs abolishes SSI also in PCs (CB$_2$R WT: ΔV_m: -6.1 ± 1.7 mV; CB$_2$R WT: ΔV_m: -0.5 ± 0.6 mV; Suppl. Fig. 2).

Finally, we tested the specificity of the CB$_2$R agonist HU-308 for inducing a long-lasting hyperpolarization in RSNPCs. In CB$_1$R-deficient mice as well as in their corresponding littermates, HU-308 application mimicked AP-induced SSI while it failed to hyperpolarize RSNPCs in CB$_2$R-deficient mice (Fig. 4G – I: CB$_1$R KO: ΔV_m: -4.9 ± 1.9 mV 7/10 responsive cells; CB$_1$R WT: ΔV_m: -5.5 ± 1.6 mV, 7/10 responsive cells; CB$_2$R KO: ΔV_m: 0.5 ± 1.5 mV, 0/8 responsive cells; CB$_2$R WT: ΔV_m: -4.1 ± 1.8 mV, 7/11 responsive cells). These experiments rule out potential off-target effects of HU-308 in the induction of SSI, and underlie establish its specificity for CB$_2$R at a concentration of 1 µM.

Taken together, both pharmacological intervention and genetic ablation of CB$_2$Rs confirm the involvement of CB$_2$Rs in SSI of layer 2/3 regular spiking cells, providing strong evidence that cell-autonomous activation of CB$_2$Rs and downstream GIRK channel opening is mediating the AP-induced self-inhibition in these cell types.

4 Discussion

Here, we show that trains of APs induce SSI in RSNPCs and PCs in layer 2/3 of the somatosensory cortex but not in FS interneurons. This cell type-specific expression of SSI was also described for layer 5 of the somatosensory cortex, where only LTS interneurons, but not FS neurons exhibited SSI (Bacci et al., 2004). In RSNPCs of layer 2/3 we investigated the underlying mechanism in detail using pharmacological tools as well as CB_1R- and CB_2R-deficient mice. We find that SSI is selectively mediated by CB_2Rs in both RSNPCs as well as PCs. This is somewhat unexpected as CB_1Rs have been previously implicated in SSI of PCs in layer 2/3 of somatosensory cortex (Marinelli et al., 2009).

Several recent studies have described the role of CB_2Rs in cellular auto-inhibition: In hippocampal pyramidal neurons CB_2Rs mediate SSI after trains of APs (Stempel et al., 2016). Additionally, intracellular CB_2Rs were also shown to reduce firing frequency in PCs of the prefrontal cortex (den Boon et al., 2012). Furthermore, application of CB_2R agonists hyperpolarizes dissociated dopaminergic neurons of the ventral tegmental area and inhibits spiking (Zhang et al., 2014). Together these findings illustrate that CB_2R activation can lead to modifications in excitability in several different cell types and in different brain regions.

What are the signaling events downstream of the endocannabinoid receptors that lead to SSI? So far, several mechanisms have been identified: In hippocampal PCs SSI is mediated by CB_2R-induced NBC transporter activation (Stempel et al., 2016). In contrast, CB_1R-mediated GIRK channel activation was described as the mechanism responsible for SSI in layer 2/3 PCs and layer 5 LTS interneurons (Bacci et al., 2004; Marinelli et al., 2009). In the present study, we demonstrate a different pathway for SSI in RSNPCs of layer 2/3 and show that APs lead to the activation of CB_2Rs, resulting in the opening of GIRK channels and hyperpolarization of the membrane potential.

In addition to the cell type-specific preference for endocannabinoid receptor subtypes in SSI activation, divergent intracellular transduction pathways are also employed to hyperpolarize the membrane potential. Given the variability of receptor and receptor subtype expression across different classes of neurons, it is not surprising that multiple mechanisms and downstream signaling cascades are involved in phenomena such as SSI (Arey, 2014). Further, several studies have shown that CB_2Rs activation can lead to selective utilization of different transduction pathways (Atwood et al., 2012; Dhopeshwarkar and Mackie, 2016). Thus, cell type specific variations of the intracellular signaling machinery may determine which transduction pathway is implemented after agonist binding.

Due to the low CB_2R expression levels in neuronal cells under physiological conditions, it has been a challenging task to study CNS effects of CB_2R. Unspecific CB_1R-pharmacology (Stempel et al., 2016) and CB_2R antibodies of insufficient specificity (Cécyre et al., 2014; Marchalant et al., 2014) have previously impeded a convincing discrimination between CB_1R- and CB_2R-mediated effects in the CNS. However, in recent years, evidence accumulated suggesting that both CB_1- and CB_2Rs serve divergent physiological effects. Stempel et al. (Stempel et al., 2016) and Chen et al. (Chen et al., 2017) proposed that CB_1Rs seem to be mainly involved in modulation of synaptic functions while CB_2R activation results in postsynaptic inhibition. Additionally, microglial CB_2R expression was shown to be involved and upregulated in a variety of pathological conditions including neuroinflammation (Carlisle et al., 2002; Zoppi et al., 2014), stroke (Yu et al., 2015; Zarruk et al., 2012), Parkinson's disease (Concannon et al., 2016, 2015), Alzheimer's (Benito et al., 2003) and Huntington's disease (Palazuelos et al., 2009). Also, neuronal CB_2R expression is increased in neuropathic pain (Svíženská et al., 2013) and drug addiction (Zhang et al., 2016). Manipulation of CB_2R expression in CA1 PC or microglia was shown to induce distinct behavioral phenotypes in mice: while microglial CB_2Rs

were involved in contextual fear memory, overexpression or disruption of CB_2Rs in PC lowered anxiety levels or enhanced spatial working memory, respectively (Li and Kim, 2017). Moreover, constitutive deletion of CB_2Rs induces a schizophrenic phenotype in mice (Ortega-Alvaro et al., 2011), increases aggressive behavior (Rodríguez-Arias et al., 2015) and modulates drug-seeking behavior for ethanol (Ortega-Álvaro et al., 2015) and nicotine (Navarrete et al., 2013). Furthermore, neuronal CB_2Rs modulate oscillatory activity – more specific theta-gamma-coupling – in the hippocampal formation (Stempel et al., 2016).

According to these data, Pacher and Machoulam (Pacher and Mechoulam, 2011) suggested that CB_2R signaling might represent a protective system that prevents tissue and cell damage. In line with this, the CB_2R mediated auto-inhibition described here may represent a cell-autonomous feedback loop preventing neurons from damage due to excessive excitability. In this study, the SSI-induced hyperpolarization is indiscriminately observed in both types of regular spiking neurons. In contrast, fast spiking interneurons do not show this phenomenon, which argues in favor of a protective role against intolerable amounts of excitation. In addition, on a more speculative note, it is likely that RSNPCS belong to a group of interneurons ($5\text{-}HT_{3A}$ receptor containing), which preferentially synapse onto other interneurons (Tremblay et al., 2016). Thus, silencing RSPNCs would lead to disinhibition of interneurons, effectively adding to the excitation protection of PCs. The long-term stability of SSI after induction is a further indication that it might occur in specific events where neurons must be prevented from excessive activity levels for a longer period of time.

In terms of the physiological relevance of the phenomenon under study, it has been shown before that SSI can also be induced with more naturally spaced activity patterns than the induction patterns used in this study: physiological spike trains from *in vivo*

recordings were applied in slices and induced SSI in CA3 pyramidal neurons of similar magnitude like the more artificial AP trains (Stempel et al., 2016). Similarly, Marinelli et al. could reliably induce SSI in cortical PC with spike trains of lower (10 – 50 Hz) frequencies (Marinelli et al., 2009). In this context it is noteworthy that for somatosensory cortex layer 2/3 regular spiking pyramidal neurons, firing frequencies of up to 60 Hz have been reported (Kinnischtzke et al., 2012). Therefore, SSI can already be induced by activity patterns of neurons that can occur *in vivo*. However, the specific role of SSI under physiological conditions has to be addressed experimentally in more detail.

Together with the lack of psychoactive effects upon CB_2R activation and other CB_1R activation-related side effects (Pertwee, 2012), these findings highlight that CB_2Rs represent an excellent target for drug-discovery research for multiple pathological conditions.

5. Conclusion

Our study describes a new mechanism by which SSI is implemented in neocortical neurons. We show that CB_2R activation leads to a GIRK channel mediated cell-autonomous hyperpolarization and provide further evidence for functional CB_2Rs in the CNS and supporting their role in regulation of neuronal excitability. Future studies combining different techniques will aid in disentangling the different roles of CB_1Rs and CB_2Rs, resulting in a better understanding of their functions and helping the discovery of specific therapeutic targets for different pathological conditions.

Acknowledgments

References

Arey, B.J., 2014. Biased Signaling in Physiology, Pharmacology and Therapeutics. Elsevier Academic Press, Amsterdam (Netherlands). https://doi.org/10.1016/B978-0-12-411460-9.00012-4

Atwood, B.K., Wager-Miller, J., Haskins, C., Straiker, A., Mackie, K., 2012. Functional selectivity in CB2 cannabinoid receptor signaling and Regulation: Implications for the Therapeutic Potential of CB2 ligands. Mol. Pharmacol. 81, 250–63. https://doi.org/10.1124/mol.111.074013

Bacci, A., Huguenard, J.R., Prince, D.A., 2004. Long-Lasting self-inhibition of neocortical interneurons mediated by endocannabinoids. Nature 431, 312–316. https://doi.org/10.1038/nature02782.1.

Benito, C., Núñez, E., Tolón, R.M., Carrier, E.J., Rábano, A., Hillard, C.J., Romero, J., 2003. Cannabinoid CB2 receptors and fatty acid amide hydrolase are selectively overexpressed in neuritic plaque-associated glia in Alzheimer's disease brains. J. Neurosci. 23, 11136–11141. https://doi.org/23/35/11136 [pii]

Buckley, N.E., McCoy, K.L., Mezey, É., Bonner, T., Zimmer, A., Felder, C.C., Glass, M., Zimmer, A., 2000. Immunomodulation by cannabinoids is absent in mice deficient for the cannabinoid CB2receptor. Eur. J. Pharmacol. 396, 141–149. https://doi.org/10.1016/S0014-2999(00)00211-9

Carlisle, S.J., Marciano-Cabral, F., Staab, A., Ludwick, C., Cabral, G.A., 2002. Differential expression of the CB2 cannabinoid receptor by rodent macrophages and macrophage-like cells in relation to cell activation. Int. Immunopharmacol. 2, 69–82. https://doi.org/10.1016/S1567-5769(01)00147-3

Cécyre, B., Thomas, S., Ptito, M., Casanova, C., Bouchard, J.F., 2014. Evaluation of the specificity of antibodies raised against cannabinoid receptor type 2 in the mouse retina. Naunyn. Schmiedebergs. Arch. Pharmacol. 387, 175–184. https://doi.org/10.1007/s00210-013-0930-8

Chen, D., Gao, M., Gao, F., Su, Q., Wu, J., 2017. Brain cannabinoid receptor 2: expression, function and modulation. Acta Pharmacol. Sin. 38, 312–316. https://doi.org/10.1038/aps.2016.149

Chevaleyre, V., Castillo, P.E., 2003. Heterosynaptic LTD of hippocampal GABAergic synapses: A novel role of endocannabinoids in regulating excitability. Neuron 38, 461–472. https://doi.org/10.1016/S0896-6273(03)00235-6

Concannon, R.M., Okine, B.N., Finn, D.P., Dowd, E., 2016. Upregulation of the cannabinoid CB2 receptor in environmental and viral inflammation-driven rat models of Parkinson's disease. Exp. Neurol. 283, 204–212. https://doi.org/10.1016/j.expneurol.2016.06.014

Concannon, R.M., Okine, B.N., Finn, D.P., Dowd, E., 2015. Differential upregulation of the cannabinoid CB2 receptor in neurotoxic and inflammation-driven rat models of Parkinson's disease. Exp. Neurol. 269, 133–141. https://doi.org/10.1016/j.expneurol.2015.04.007

den Boon, F.S., Chameau, P., Schaafsma-Zhao, Q., van Aken, W., Bari, M., Oddi, S., Kruse, C.G., Maccarrone, M., Wadman, W.J., Werkman, T.R., 2012. Excitability of prefrontal cortical pyramidal neurons is modulated by activation of intracellular type-2 cannabinoid receptors. Proc. Natl. Acad. Sci. U. S. A. 109, 3534–9. https://doi.org/10.1073/pnas.1118167109

Dhopeshwarkar, A., Mackie, K., 2016. Functional Selectivity of CB2 Cannabinoid Receptor Ligands at a Canonical and Noncanonical Pathway. J. Pharmacol. Exp. Ther. 358, 342–351. https://doi.org/10.1124/jpet.116.232561

Feng, L., Zhao, T., Kim, J., 2015. neuTube 1.0: A New Design for efficient Neuron reconstruction Software Based on the SWC Format. eNeuro 2, 1–10. https://doi.org/10.1523/JNEUROSCI.2055-07.2007

García-Gutiérrez, M.S., García-Bueno, B., Zoppi, S., Leza, J.C., Manzanares, J., 2012. Chronic blockade of cannabinoid CB 2 receptors induces anxiolytic-like actions associated with alterations in GABA A receptors. Br. J. Pharmacol. 165, 951–964. https://doi.org/10.1111/j.1476-5381.2011.01625.x

García-Gutiérrez, M.S., Ortega-Álvaro, A., Busquets-García, A., Pérez-Ortiz, J.M., Caltana, L., Ricatti, M.J., Brusco, A., Maldonado, R., Manzanares, J., 2013. Synaptic plasticity alterations associated with memory impairment induced by deletion of CB2 cannabinoid receptors. Neuropharmacology 73, 388–396. https://doi.org/10.1016/j.neuropharm.2013.05.034

Gerdeman, G.L., Ronesi, J., Lovinger, D.M., 2002. Postsynaptic endocannabinoid release is critical to long-term depression in the striatum. Nat. Neurosci. 5, 446–451. https://doi.org/10.1038/nn832

Gómez-Gonzalo, M., Navarrete, M., Perea, G., Covelo, A., Martín-Fernández, M., Shigemoto, R., Luján, R., Araque, A., 2015. Endocannabinoids induce lateral long-term potentiation of transmitter release by stimulation of gliotransmission. Cereb. Cortex 25, 3699–3712.

https://doi.org/10.1093/cercor/bhu231

Gong, J.P., Onaivi, E.S., Ishiguro, H., Liu, Q.R., Tagliaferro, P.A., Brusco, A., Uhl, G.R., 2006. Cannabinoid CB2 receptors: Immunohistochemical localization in rat brain. Brain Res. 1071, 10–23. https://doi.org/10.1016/j.brainres.2005.11.035

Hanus, L., Abu-Lafi, S., Fride, E., Breuer, A., Vogel, Z., Shalev, D.E., Kustanovich, I., Mechoulam, R., 2001. 2-Arachidonyl glyceryl ether, an endogenous agonist of the cannabinoid CB1 receptor. Proc. Natl. Acad. Sci. 98, 3662–3665. https://doi.org/10.1073/pnas.061029898

Kano, M., 2009. Endocannabinoid-mediated control of synaptic transmission. Physiol Rev 89, 309–380. https://doi.org/10.1152/physrev.00019.2008.

Kim, J., Li, Y., 2015. Chronic activation of CB2 cannabinoid receptors in the hippocampus increases excitatory synaptic transmission. J. Physiol. 593, 871–886. https://doi.org/10.1113/jphysiol.2014.286633

Kinnischtzke, A.K., Sewall, A.M., Berkepile, J.M., Fanselow, E.E., 2012. Postnatal maturation of somatostatin-expressing inhibitory cells in the somatosensory cortex of GIN mice. Front. Neural Circuits 6, 1-12. https://doi:10.3389/fncir.2012.00033

Kreitzer, a C., Regehr, W.G., 2001. Cerebellar depolarization-induced suppression of inhibition is mediated by endogenous cannabinoids. J. Neurosci. 21, RC174. https://doi.org/20015720 [pii]

Li, Y., Kim, J., 2017. Distinct roles of neuronal and microglial CB2 cannabinoid receptors in the mouse hippocampus. Neuroscience 363, 11–25. https://doi.org/10.1016/j.neuroscience.2017.08.053

Maglio, L.E., Noriega-Prieto, J.A., Maraver, M.J., Fernández de Sevilla, D., 2017. Endocannabinoid-Dependent Long-Term Potentiation of Synaptic Transmission at Rat Barrel Cortex. Cereb. Cortex 1–14. https://doi.org/10.1093/cercor/bhx053

Marchalant, Y., Brownjohn, P.W., Bonnet, A., Kleffmann, T., Ashton, J.C., 2014. Validating Antibodies to the Cannabinoid CB2 Receptor: Antibody Sensitivity Is Not Evidence of Antibody Specificity. J. Histochem. Cytochem. 62, 395–404. https://doi.org/10.1369/0022155414530995

Marinelli, S., Pacioni, S., Cannich, A., Marsicano, G., Bacci, A., 2009. Self-modulation of neocortical pyramidal neurons by endocannabinoids. Nat. Neurosci. 12, 1488–1490. https://doi.org/10.1038/nn.2430

Munro, S., Thomas, K.L., Abu-Shaar, M., 1993. Molecular characterization of a peripheral receptor for cannabinoids. Nature 365, 61–65. https://doi.org/10.1038/365061a0

Navarrete, F., Rodríguez-Arias, M., Martín-García, E., Navarro, D., García-Gutiérrez, M.S., Aguilar, M.A., Aracil-Fernández, A., Berbel, P., Miñarro, J., Maldonado, R., Manzanares, J., 2013. Role of CB2 cannabinoid receptors in the rewarding, reinforcing, and physical effects of nicotine. Neuropsychopharmacology 38, 2515–2524. https://doi.org/10.1038/npp.2013.157

Ohno-Shosaku, T., Maejima, T., Kano, M., 2001. Endogenous cannabinoids mediate retrograde signals from depolarized postsynaptic neurons to presynaptic terminals. Neuron 29, 729–738. https://doi.org/10.1016/S0896-

6273(01)00247-1

Onaivi, E.S., 2007. Neuropsychobiological evidence for the functional presence and expression of cannabinoid CB2 receptors in the brain. Neuropsychobiology 54, 231–246. https://doi.org/10.1159/000100778

Ortega-Alvaro, A., Aracil-Fernández, A., García-Gutiérrez, M.S., Navarrete, F., Manzanares, J., 2011. Deletion of CB2 Cannabinoid Receptor Induces Schizophrenia-Related Behaviors in Mice. Neuropsychopharmacology 36, 1489–1504. https://doi.org/10.1038/npp.2011.34

Ortega-Álvaro, A., Ternianov, A., Aracil-Fernández, A., Navarrete, F., García-Gutiérrez, M.S., Manzanares, J., 2015. Role of cannabinoid CB2receptor in the reinforcing actions of ethanol. Addict. Biol. 20, 43–55. https://doi.org/10.1111/adb.12076

Pacher, P., Mechoulam, R., 2011. Is lipid signaling through cannabinoid 2 receptors part of a protective system? Prog. Lipid Res. 50, 193–211. https://doi.org/10.1016/j.plipres.2011.01.001

Palazuelos, J., Aguado, T., Pazos, M.R., Julien, B., Carrasco, C., Resel, E., Sagredo, O., Benito, C., Romero, J., Azcoitia, I., Fernández-Ruiz, J., Guzmán, M., Galve-Roperh, I., 2009. Microglial CB2cannabinoid receptors are neuroprotective in Huntington's disease excitotoxicity. Brain 132, 3152–3164. https://doi.org/10.1093/brain/awp239

Pertwee, R.G., 2012. Targeting the endocannabinoid system with cannabinoid receptor agonists: pharmacological strategies and therapeutic possibilities. Philos. Trans. R. Soc. B Biol. Sci. 367, 3353–3363. https://doi.org/10.1098/rstb.2011.0381

Rodríguez-Arias, M., Navarrete, F., Blanco-Gandia, M.C., Arenas, M.C., Aguilar, M.A., Bartoll-Andrés, A., Valverde, O., Miñarro, J., Manzanares, J., 2015. Role of CB2 receptors in social and aggressive behavior in male mice. Psychopharmacology (Berl). 232, 3019–3031. https://doi.org/10.1007/s00213-015-3939-5

Safo, P.K., Regehr, W.G., 2005. Endocannabinoids control the induction of cerebellar LTD. Neuron 48, 647–659. https://doi.org/10.1016/j.neuron.2005.09.020

Schindelin, J., Arganda-Carreras, I., Frise, E., Kaynig, V., Longair, M., Pietzsch, T., Preibisch, S., Rueden, C., Saalfeld, S., Schmid, B., Tinevez, J.-Y.J.-Y., White, D.J., Hartenstein, V., Eliceiri, K., Tomancak, P., Cardona, A., Liceiri, K., Tomancak, P., A., C., 2012. Fiji: An open source platform for biological image analysis. Nat. Methods 9, 676–682. https://doi.org/10.1038/nmeth.2019.Fiji

Sjöström, P.J., Turrigiano, G.G., Nelson, S.B., 2003. Neocortical LTD via coincident activation of presynaptic NMDA and cannabinoid receptors. Neuron 39, 641–654. https://doi.org/10.1016/S0896-6273(03)00476-8

Stempel, A.V., Stumpf, A., Zhang, H.Y., Özdoğan, T., Pannasch, U., Theis, A.K., Otte, D.M., Wojtalla, A., Rácz, I., Ponomarenko, A., Xi, Z.X., Zimmer, A., Schmitz, D., 2016. Cannabinoid Type 2 Receptors Mediate a Cell Type-Specific Plasticity in the Hippocampus. Neuron 90, 795–809. https://doi.org/10.1016/j.neuron.2016.03.034

Svíženská, I.H., Brázda, V., Klusáková, I., Dubový, P., 2013. Bilateral Changes of Cannabinoid Receptor Type 2 Protein and mRNA in the Dorsal Root Ganglia

of a Rat Neuropathic Pain Model. J. Histochem. Cytochem. 61, 529–547. https://doi:10.1016/j.neuron.2016.06.033

Tremblay, R., Soohyun. L., Rudy, B., 2016. GABAergic Interneurons in the Neocortex: From Cellular Properties to Circuits. Neuron 91, 260-292 https://doi.org/10.1016/j.neuron.2016.03.034

Wang, W., Trieu, B.H., Palmer, L.C., Jia, Y., Pham, D.T., Jung, K.-M., Karsten, C.A., Merrill, C.B., Mackie, K., Gall, C.M., Piomelli, D., Lynch, G., 2016. A Primary Cortical Input to Hippocampus Expresses a Pathway-Specific and Endocannabinoid-Dependent Form of Long-Term Potentiation. eNeuro 3, 160–16. https://doi.org/10.1523/ENEURO.0160-16.2016

Wilson, R.I., Nicoll, R. a, 2001. Endogenous cannabinoids mediate retrograde signalling at hippocampal synapses. Nature 410, 588–592. https://doi.org/10.1038/35069076

Yu, S.J., Reiner, D., Shen, H., Wu, K.J., Liu, Q.R., Wang, Y., 2015. Time-dependent protection of CB2 receptor agonist in stroke. PLoS One 10, 1–17. https://doi.org/10.1371/journal.pone.0132487

Zarruk, J.G., Fernández-López, D., García-Yébenes, I., García-Gutiérrez, M.S., Vivancos, J., Nombela, F., Torres, M., Burguete, M.C., Manzanares, J., Lizasoain, I., Moro, M.A., 2012. Cannabinoid type 2 receptor activation downregulates stroke-induced classic and alternative brain macrophage/microglial activation concomitant to neuroprotection. Stroke 43, 211–219. https://doi.org/10.1161/STROKEAHA.111.631044

Zhang, H.-Y., Gao, M., Liu, Q.-R., Bi, G.-H., Li, X., Yang, H.-J., Gardner, E.L., Wu, J., Xi, Z.-X., 2014. Cannabinoid CB2 receptors modulate midbrain dopamine neuronal activity and dopamine-related behavior in mice. Proc. Natl. Acad. Sci. U. S. A. 111, E5007-5015. https://doi.org/10.1073/pnas.1413210111

Zhang, H.-Y., Gao, M., Shen, H., Bi, G.-H., Yang, H.-J., Liu, Q.-R., Wu, J., Gardner, E.L., Bonci, A., Xi, Z.-X., 2016. Expression of functional cannabinoid CB2 receptor in VTA dopamine neurons in rats. Addict. Biol. 22, 752–765. https://doi.org/10.1111/adb.12367

Zimmer, a M., Hohmann, a G., Herkenham, M., Bonner, T.I., 1999. Increased mortality, hypoactivity, and hypoalgesia in cannabinoid CB1 receptor knockout mice. Proc. Natl. Acad. Sci. U. S. A. 96, 5780–5785. https://doi.org/10.1073/pnas.96.10.5780

Zoppi, S., Madrigal, J.L., Caso, J.R., García-Gutiérrez, M.S., Manzanares, J., Leza, J.C., García-Bueno, B., 2014. Regulatory role of the cannabinoid CB2 receptor in stress-induced neuroinflammation in mice. Br. J. Pharmacol. 171, 2814–2826. https://doi.org/10.1111/bph.12607

Fig. 1. Trains of APs induce cell type-specific hyperpolarization in regular firing neurons in layer II/III of somatosensory cortex.

A – C) Characteristic cell morphology and firing pattern of a PC (A), an RSNPC (B) and a FS interneuron (C), visualized by post-hoc biocytin staining and reconstruction. Scale bar: 50 μm; arrow heads depict the direction of the pial surface. Insets show neuron-type-specific firing patterns evoked by depolarizing current injection (scale bars: 20 mV, 0.2 s).

D – I) Single cell examples (D – F) and time course of the average membrane potential (G – I) before, during and after ten trains of APs (black lines) in the different cell types.

J – L) Individual magnitudes of the AP-train induced hyperpolarization. Trains of APs induce SSI in PCs (D, G, J; n = 11) and in RSNPCs (E, H, K; n = 21), but not in FS interneurons (F, I, L; n = 6).

Fig. 2. AP-induced hyperpolarization is accompanied by a reduction in input resistance that is mediated by activation of GIRK-channels in RSNPCs.

A) The amplitude of the hyperpolarization (ΔV_m) correlates with the reduction in input resistance (normalized to the pre-AP average; r^2 = 0.81, p < 0.0001). Inset: example traces of -40 pA testpulses before and after AP trains; scale bars: 0.2 s, 5 mV; filled circle in the plot depicts example recording.

B) Inhibition of AP-induced hyperpolarization by preincubation with the GIRK channel blocker SCH23390 (10 µM; B; black lines mark AP stimulation). C) SCH23390 reduced the average SSI magnitude (*** p = 0.0005, Student's t-test; control n = 21; SCH23390 n = 11) as well as percentage of hyperpolarizing cells (D).

E) Single cell example of the depolarization induced by application of SCH23390 (10 µM) after AP-induced SSI, compared to a control recording without SCH23390 application.

F) Summary of the SCH23390 effect on the membrane potential after SSI induction (n = 5).

G) Application of SCH2330 on non-stimulated cells (on baseline) causes only a minor depolarization (* p = 0.0159 Mann-Whitney test; on baseline: n = 4; after SSI: n = 5) compared to the effect after SSI.

Fig. 3. Pharmacological experiments indicate involvement of CB$_2$R in RSNPC SSI.

A) Time course of the average membrane potential in response to application of the specific CB$_2$R agonist HU-308 (1 µM) and the endocannabinoid NE (300 nM) that displays a selectivity for CB$_1$Rs over CB$_2$Rs. Agonist application is indicated by the black line.

B) Individual magnitudes of agonist-induced hyperpolarization. NE does not cause a hyperpolarization (** p = 0.005, Mann-Whitney rest; HU-308: n = 10; NE: n = 11).

C) Time course of the average membrane potential before, during (black lines) and after AP trains in presence or absence of the CB$_2$R inverse agonist SR 144528 (1 µM).

D) Individual magnitudes of AP-induced hyperpolarization in the presence of SR 144528. Preincubation with SR 144528 prevents AP-induced hyperpolarization (** p = 0.0019, Mann-Whitney rest; SR 144528: n = 15; control: n = 21).

Fig. 4. AP-induced hyperpolarization in RSNPCs is absent in CB$_2$R-deficient mice but present in CB$_1$R-deficient mice.

A − C) AP-induced SSI in RSNPCs of CB$_1$R-deficient mice is indistinguishable from SSI in WT-littermates (p = 0.4 Student's t-test; CB$_1$R KO n = 17; CB$_1$R WT n = 10). A) Time course of the average membrane potential in WT (open circles) and CB$_1$R KO mice (black circles). B) Overview on individual magnitudes of AP-induced hyperpolarization. C) Percentage of cells in which AP trains evoked hyperpolarization. AP trains are indicated by black bars.

D − F) Trains of APs failed to induced SSI in CB$_2$R-deficient mice compared to WT-littermates (** p = 0.0029 Student's t-test; CB$_2$R KO n = 12; CB$_2$R WT n = 12). D) Time
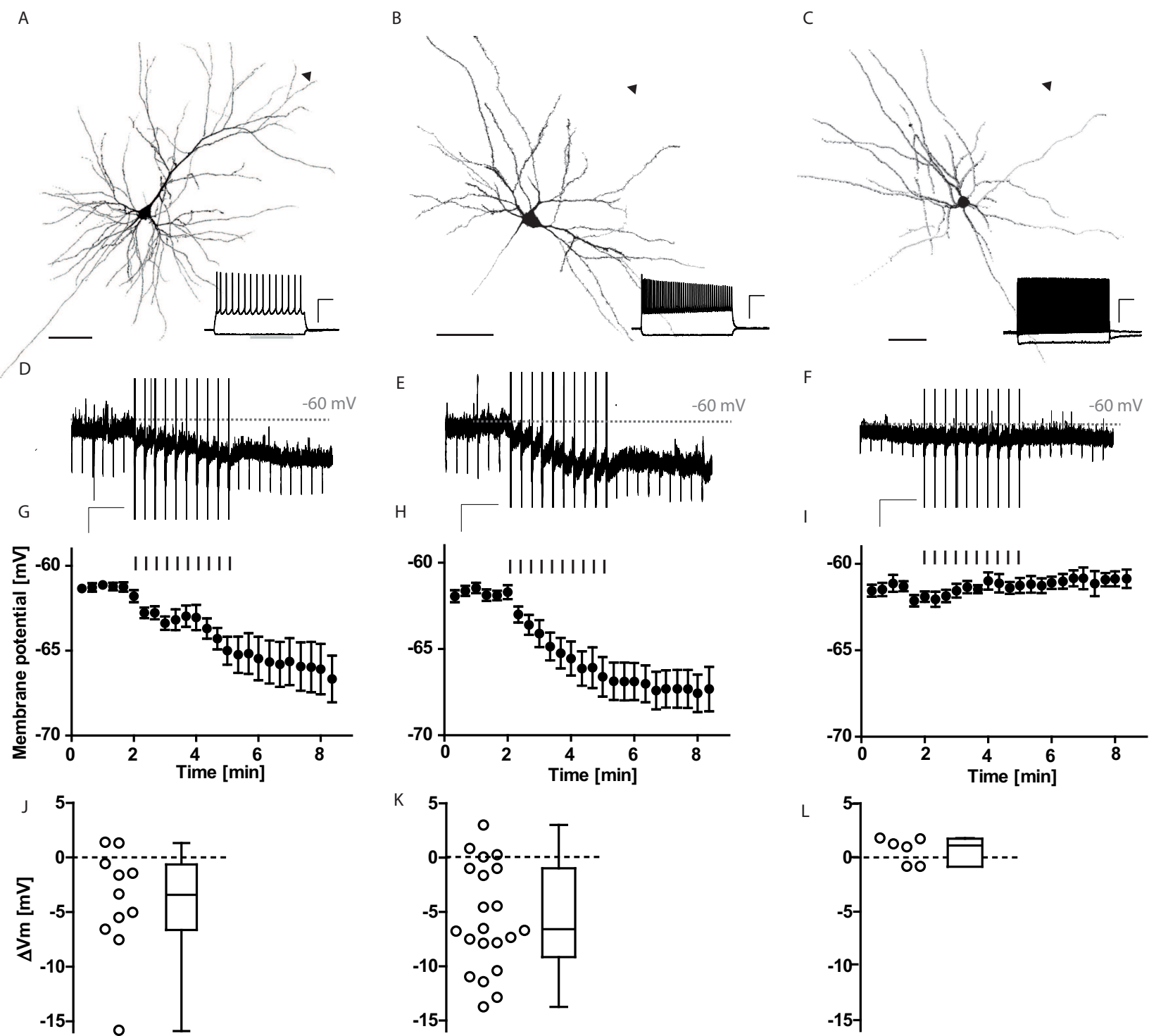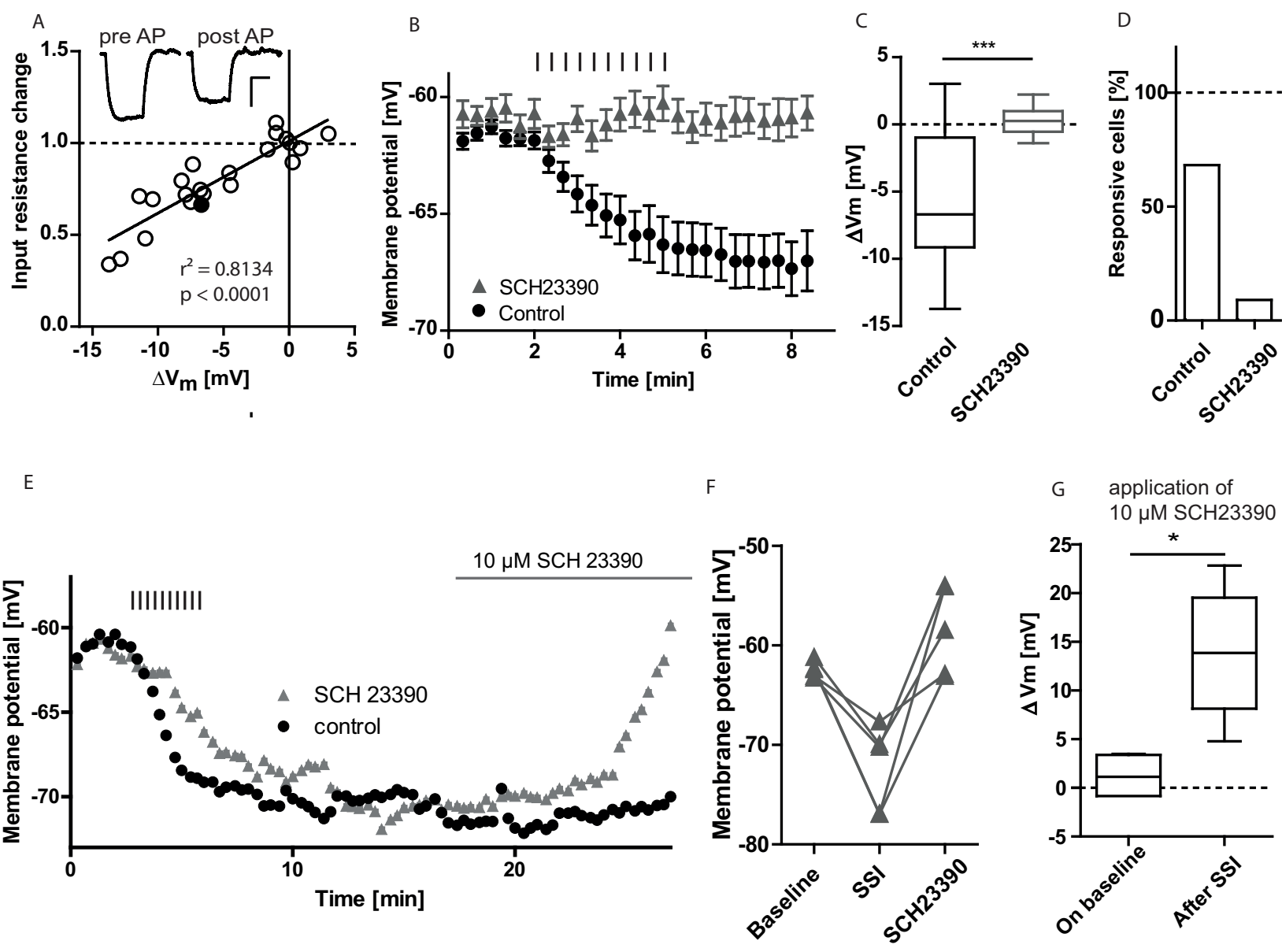
course of the average membrane potential in WT (open circles) and CB_2R KO mice (black circles). E) Individual magnitudes of the AP-induced hyperpolarization. F) Percentage of cells in which AP trains evoked a hyperpolarization. AP trains are indicated by black bars.

G – I) HU-308 (1 µM) hyperpolarized RSNPCs in CB_1R deficient mice and WT-littermates of transgenic animals (p = 0.8 Student's t-test; CB_1R KO n = 10; CB_1R WT n = 10), but not in CB_2R-deficient mice (* p = 0.046; CB_2R KO n = 8; CB_2R WT n = 11). G) Exemplary time course of the membrane potential of RSNPCs in response to HU-308 application (black line). Note the hyperpolarization in the CB_1R KO (black circles), and the lack of hyperpolarization in the CB_2R KO (black squares). H) Individual magnitudes of agonist-induced hyperpolarization in different genotypes. I) Percentage of cells in which agonist application evoked hyperpolarization.

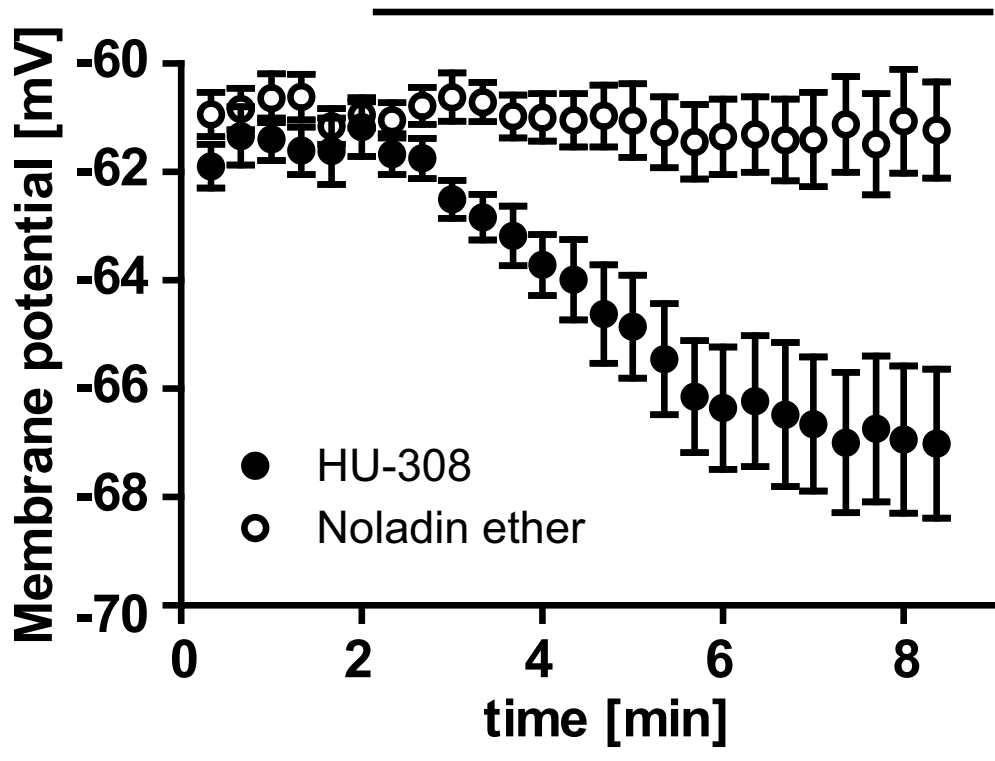**Table 1: cell properties of cortical neurons in somatosensory cortex layer 2/3**

	PCs (11)	RSNPCs (21)	FSs (6)
Resting membrane potential [mV]	-81.9 ± 2.0	-80.6 ± 1.2	-65.2 ± 1.9
Input resistance [MΩ]	153.1 ± 11.6	189.3 ± 13.87	80,6 ± 9.7
AP half-width [ms]	1.0 ± 0.08	1.6 ± 0.1	0.3 ± 0.19
AP threshold [mV]	-33.9 ± 1.3	-36.0 ± 1.0	-46.8 ± 2.6
AP slope ratio	4.5 ± 0.2	4.5 ± 0.2	0.9 ± 0.1
AHP [mV]	-16.7 ± 0.7	-15.0 ± 0.5	-18.1 ± 0.6
Maximal firing frequency [Hz]	36.8 ± 2.3	41.17 ± 2.3	360 ± 39.9

Values are given as mean ± SEM, PC: pyramidal cell; RSNPC: regular spiking non-pyramidal cell; FS: fast spiking interneuron; AHP: Afterhyperpolarization; numbers of recorded cells are displayed in parentheses.
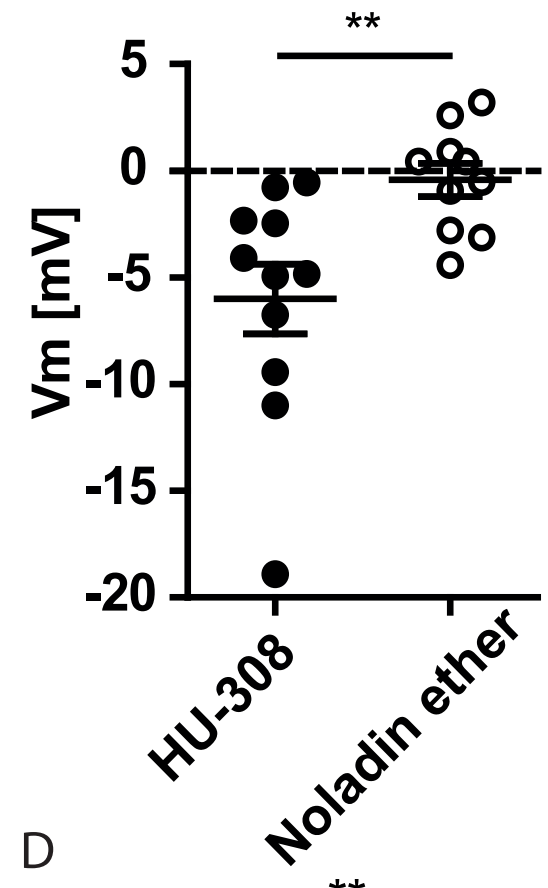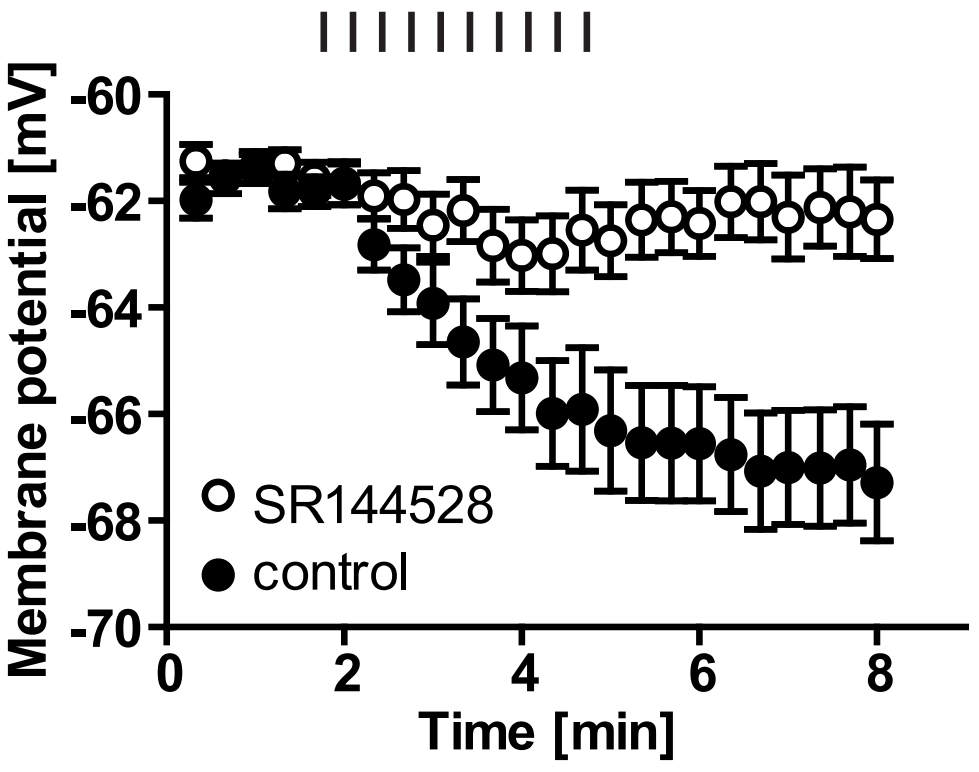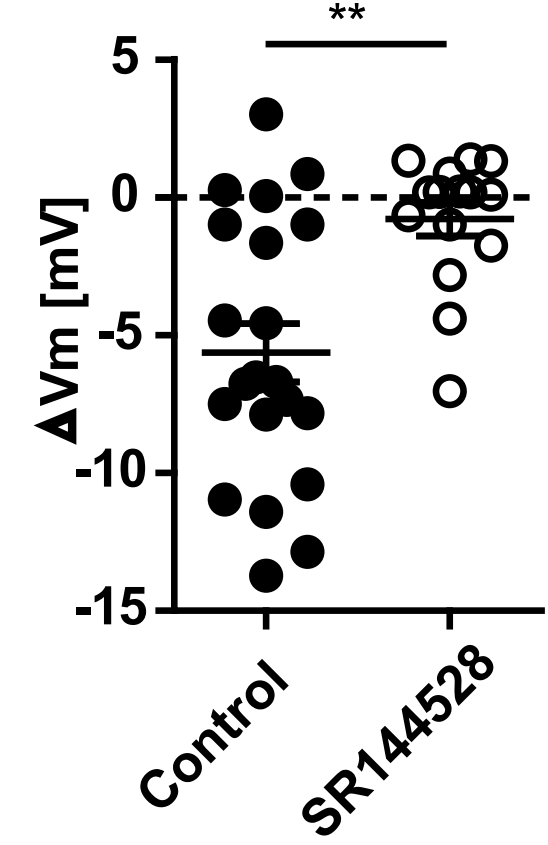
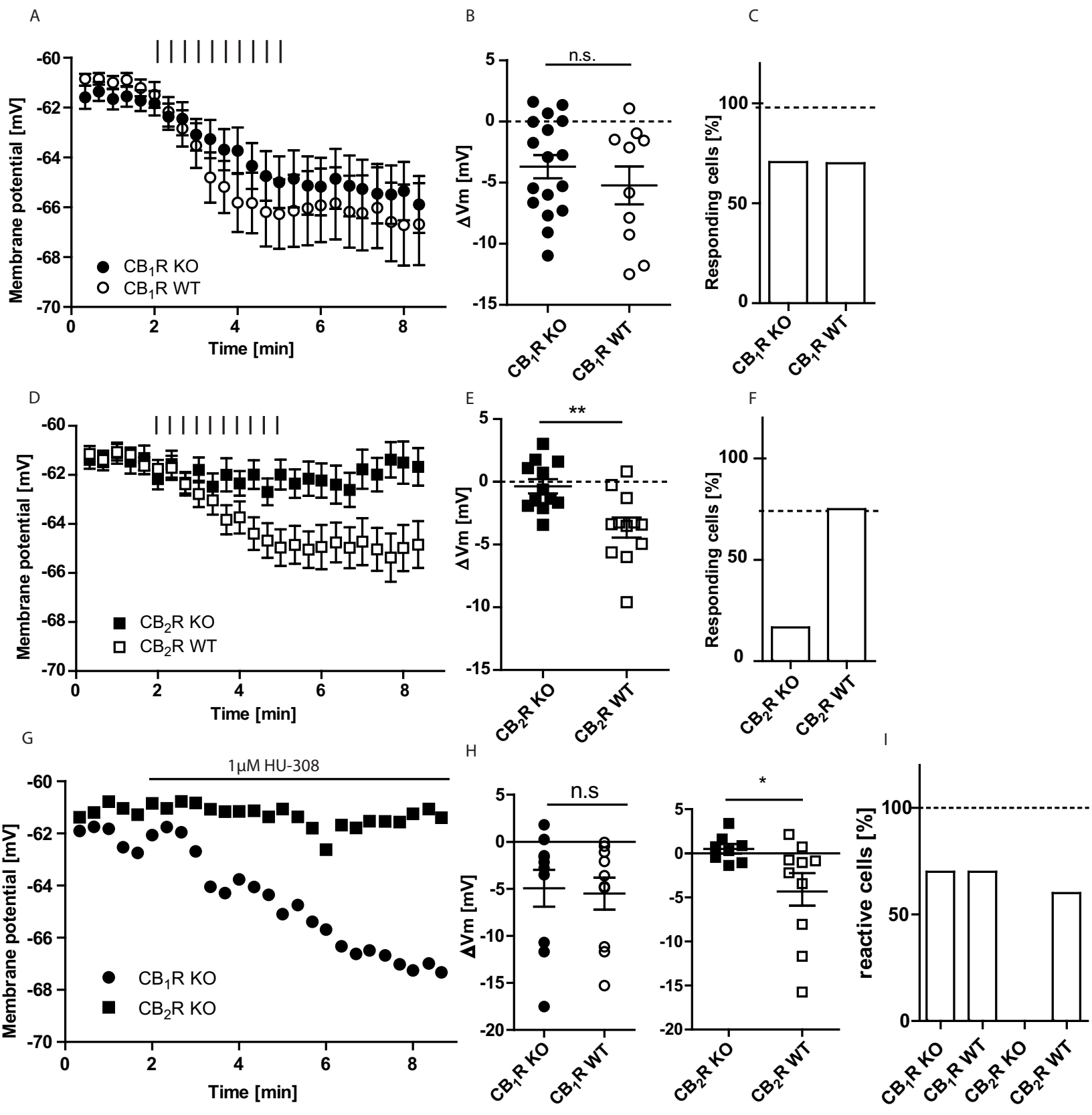**Supplementary Material**